Inorg. Chem. **2008**, *47*, 3166−3172

Reactivity of an Aminopyridine $[LMn^{II}]^{2+}$ Complex with H_2O_2. Detection of Intermediates at Low Temperature

Sihem Groni,[†] Pierre Dorlet,[†,‡] Guillaume Blain,[§] Sophie Bourcier,[⊥] Régis Guillot,[§] and Elodie Anxolabéhère-Mallart*,[†]

Institut de Chimie Moléculaire et des Matériaux d'Orsay, UMR CNRS 8182, Equipe de Chimie Inorganique, Université Paris XI, 91405 Orsay, France, Laboratoire du Stress Oxydant et Détoxication, URA CNRS 2096-IBITECS CEA Saclay, Bat. 532, 91191 Gif-sur-Yvette Cedex, France, Institut de Chimie Moléculaire et des Matériaux d'Orsay, UMR CNRS 8182, Université Paris XI, 91405 Orsay, France, and Ecole Polytechnique 91128 Palaiseau, France

Received November 14, 2007

In the present work we report the reactivity of $[LMn^{II}]^{2+}$ toward addition of hydrogen peroxide (H_2O_2) in acetonitrile solution, where L is a pentadentate polypyridine ligand. Formation of peroxo complexes is evidenced by low-temperature UV–visible spectroscopy, ESI-mass spectrometry, and EPR spectroscopy using parallel as well as perpendicular mode detection. The influence of the medium (basicity, water content) on the formation of various species is investigated. In basic nonanhydrous medium the fate of the reaction mixture solution is the formation of the di-μ-oxo mixed-valent Mn(III)Mn(IV) dinuclear complex. In acidic medium the building of the oxo bridges is avoided and the reaction mixture evolves toward oxidation of the ligand L. This reaction route offers new opportunities for the study of oxidation reactivity of Mn (hydro)peroxo complexes.

Introduction

Metal−hydroxo(oxo) and metal−peroxo complexes are of interest because of their presence in many enzymatic reactions[1,2] as well as in catalytic oxygenation reactions as key intermediates.[2,3] Following the bioinorganic approach, chemists have made important strides in the synthesis and characterization by various spectroscopic methods of metal−O_2 adducts and investigated their reactivities in the oxidation of organic substrates.[4–8] Both iron and copper model compounds have been extensively studied, and numerous examples of peroxoiron(III) complexes with heme and non-heme ligands have been synthesized as chemical models of cytochrome P450 or dioxygenases[6] as well as peroxocopper(III).[7,8] More recently peroxonickel(III) complexes have been reported in the literature.[9,10] Mn−peroxo-(hydroperoxo) intermediates have also been invoked as reactive intermediate in the reactions of Mn-containing enzymes such as MnSOD,[11] catalase,[12] and the oxygen-evolving complex of Photosystem II.[13–17] Few examples of Mn(III) peroxo complexes have been reported in the literature. The first X-ray crystal structure was the Mn(III) peroxo porphyrin complex $[Mn^{III}(TPP)(O_2)]^-$ (TPP = *meso*-tetraphenylporphyrin) reported by Valentine.[18] Two Mn(III) peroxo complexes were ultimately reported with the non-porphyrinic ligand Tp^{iPr2} (Tp^{iPr2} = tris(3,5-diisopropylpyra-

* To whom correspondence should be addressed. E-mail: eanxolab@icmo.u-psud.fr. Tel: +33 169153207. Fax: +33 169154754.
† UMR CNRS 8182, Université Paris XI.
‡ URA CNRS 2096-IBITECS CEA Saclay.
§ UMR CNRS 8182, Université Paris XI.
⊥ Ecole Polytechnique.

(1) Holm, R. H.; Kennepohl, P.; Solomon, E. I. *Chem. Rev.* **1996**, *96*, 2239–2314.
(2) Meunier, B. *Biomimetic Oxidation Catalysed by Transition Metal Complexes*. Imperial College Press: London, 2000.
(3) Punniyamurthy, T.; Velusamy, S.; Iqbal, J. *Chem. Rev.* **2005**, *105*, 2329–2364.
(4) Momenteau, M.; Reed, C. A. *Chem. Rev.* **1994**, *94*, 659–698.
(5) Solomon, E. I.; Brunold, T. C.; Davis, M. I.; Kemsley, J. N.; Lee, S.-K.; Lehnert, N.; Neese, F.; Skulan, A. J.; Yang, Y.-S.; Zhou, J. *Chem. Rev.* **2000**, *100*, 235–349.
(6) Costas, M.; Mehn, M. P.; Jensen, M. P.; Que, L. *Chem. Rev.* **2004**, *104*, 939–986.
(7) Mirica, L. M.; Ottenwaelder, X.; Stack, D. T. *Chem. Rev.* **2004**, *104*, 1013–1045.
(8) Lewis, E. A.; Tolman, W. B. *Chem. Rev.* **2004**, *104*, 1047–1076.
(9) Matsuda, K.; Irie, M. *J. Am. Chem. Soc.* **2000**, *122*, 8309–8310.
(10) Kieber-Emmons, M. T.; Annaraj, J.; Seo, M. S.; Van Heuvelen, K. M.; Tosha, T.; Kitagawa, T.; Brunold, T. C.; Nam, W.; Riordan, C. G. *J. Am. Chem. Soc.* **2006**, *128*, 14230–14231.
(11) Jackson, T. A.; Karapetian, A.; Miller, A.-F.; Brunold, T. C. *Biochemistry* **2005**, *44*, 1504–1520.
(12) Pecoraro, V. L.; Baldwin, M. J.; Gelasco, A. *Chem. Rev.* **1994**, *94*, 807–826.

10.1021/ic702238z CCC: $40.75
Published on Web 03/28/2008

Scheme 1. Ligand L

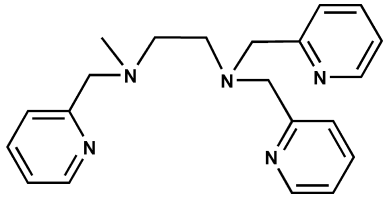

zolyl)borate).[19,20] In one case the X-ray crystal structure shows an intramolecular hydrogen-bonding interaction between the η^2-peroxide and the N−H functional group of the pyrazole ligand,[19] whereas in the other case an intermolecular hydrogen-bonding interaction between η^2-peroxide and the N−H functional group of a imidazolyl ligand was evidenced.[20] More recently Nam and co-workers reported the X-ray crystal structure of a Mn(III) side-on peroxo complex with the 4N macrocyclic tetradentate ligand tmc (tmc = 1,4,8,11-tetramethyl-1,4,8,11-tetraazacyclotetradecane) and demonstrated the reactivity of the complex toward aldehyde deformylation.[21] In our laboratory we also reported the preparation of a non-heme Mn(III) peroxo complex obtained upon addition of potassium superoxide to $[LMn^{II}]^{2+}$ (L = *N*-methyl-*N*′,*N*″-tris(2-pyridylmethyl)ethane-1,2-diamine; see Scheme 1).[22]

The $[LMn^{III}(OO)]^{+}$ species was characterized by UV–vis spectroscopy and ESI-mass spectrometry (ESI-MS) as well as parallel mode EPR spectroscopy. Indeed, EPR spectroscopy is known to be an efficient spectroscopic method to detect Mn species in various oxidation states, in model compounds as well as in natural systems.[23] Whereas conventional perpendicular mode EPR is well suited for the observation of half-integer spin systems (for example Mn(II), Mn(IV), mixed-valent Mn clusters, organic radicals), the technique of parallel polarization EPR has been used for observing EPR signals issued from an integer spin system, in particular $S = 2$.[24–26] In the case of Mn(III), Klein and co-workers were first to report that stronger signals are obtained with a geometry in which the microwave magnetic field is polarized parallel to the applied magnetic field, in contrast to the conventional EPR method in which the microwave field is polarized perpendicular to the applied field.[27] Later, parallel polarization EPR studies of Mn(III) ion in the manganese superoxide dismutase enzyme,[28] in Photosystem II,[29] and in an Mn(III) salen compound[30] demonstrated that parallel polarization mode EPR can be a powerful tool for obtaining information on zero-field splitting values or metal center geometry.

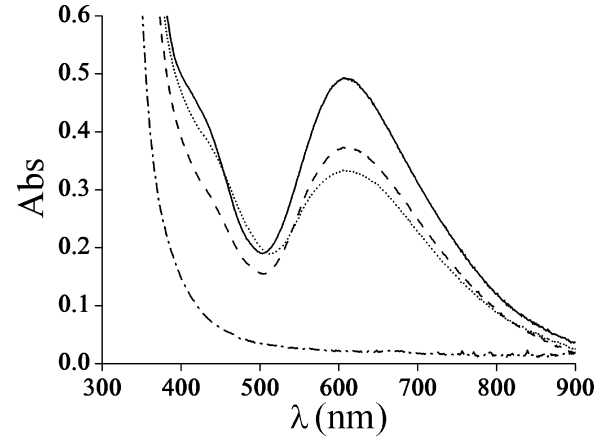

Figure 1. UV–vis spectrum of an anhydrous MeCN solution of $[LMn^{II}]^{2+}$ (5 mM) upon addition of H_2O_2 under various conditions: (• − •) initial colorless solution; (−) after the addition of 250-fold excess of H_2O_2 (35% aqueous) referred to as the blue-green solution in the text; (- - -) after addition of 2 equiv of $(Et)_3N$ to the blue-green solution; (•••) after addition of 1 equiv of H^+ ($HClO_4$) to the blue-green solution. T = – 25 °C, optical path length 1 cm.

In the present work we report the reactivity of the Mn(II) complex $[LMn^{II}]^{2+}$ with H_2O_2 in various media. The pentadentate ligand L was used (Scheme 1) in order to keep an accessible vacant position in the Mn coordination sphere. The evolution of the reaction was characterized by low-temperature UV–vis absorption spectroscopy, perpendicular mode as well as parallel mode EPR spectroscopy, and ESI-MS. The formation of monomeric Mn(III) peroxo species is evidenced by X-band EPR using parallel mode detection as well as ESI MS. The influence of the medium (basicity, water content) on the formation of various species is investigated.

Results and Discussion

In the present study a 5 mM solution of the $[LMn^{II}]^{2+}$ species was generated in situ by mixing L and $Mn^{II}(ClO_4)_2$ in acetonitrile (MeCN).[22,31] Upon addition of excess of hydrogen peroxide (H_2O_2) at −25 °C the solution changed from colorless to blue-green and O_2 evolution was observed. Figure 1 shows the evolution of the UV–vis spectrum upon

(13) Pecoraro, V. L.; Baldwin, M. J.; Caudle, M. T.; Hsieh, W.-Y.; Law, N. A. *Pure Appl. Chem.* **1998**, *70*, 925–929.
(14) Messinger, J.; Seaton, G.; Wydrzynski, T.; Wacker, U.; Renger, G. *Biochemistry* **1997**, *36*, 6862–6873.
(15) Britt, R. D.; Campbell, K. A.; Peloquin, J. M.; Gilchrist, M. L.; Aznar, C.; Dicus, M. M.; Robblee, J. H.; Messinger, J. *Biochim. Biophys. Acta: Bioenerg.* **2004**, *1655*, 158–171.
(16) Wu, A. J.; Penner-Hahn, J. E.; Pecoraro, V. L. *Chem. Rev.* **2004**, *104*, 903–938.
(17) McEvoy, J. P.; Gascón, J. A.; Batista, V. S.; Brudvig, G. W. *Photochem. Photobiol. Sci.* **2005**, *4*, 940–949.
(18) VanAtta, R. B.; Strouse, C. E.; Hanson, L. K.; Valentine, A. M. *J. Am. Chem. Soc.* **1987**, *109*, 1425.
(19) Kitajima, N.; Komatsuzaki, H.; Hikichi, S.; Osawa, M.; Moro-Oka, Y. *J. Am. Chem. Soc.* **1994**, *116*, 11596–11597.
(20) Singh, U. P.; Sharma, A. K.; Hikichi, S.; Komatsuzaki, H.; Moro-Oka, Y.; Munetaka, A. *Inorg. Chim. Acta* **2006**, *359*, 4407–4411.
(21) Seo, M. S.; Kim, J. Y.; Annaraj, J.; Kim, Y.; Lee, Y.-M.; Kim, S.-J.; Kim, J.; Nam, W. *Angew. Chem., Int. Ed.* **2007**, *46*, 377–380.
(22) Groni, S.; Blain, G.; Guillot, R.; Policar, C.; Anxolabéhère-Mallart, E. *Inorg. Chem.* **2007**, *46*(6), 1951–1953.
(23) Hagen, W. R. *Dalton Trans.* **2006**, 4415–4434.
(24) Abragam, A.; Bleaney, B., *Electron Paramagnetic Resonance of Transition Ions*, Clarendon Press: Oxford, U.K., 1970.
(25) Hendrich, M. P.; Debrunner, P. G. *J. Magn. Reson.* **1988**, *78*, 133–141.
(26) Hendrich, M. P.; Debrunner, P. G. *Biophys. J.* **1989**, *56*, 489–506.
(27) Dexheimer, S. L.; Gohdes, J. W.; Chan, M. K.; Hagen, K. S.; Armstrong, W. H.; Klein, M. P. *J. Am. Chem. Soc.* **1989**, *111*, 8923–8925.
(28) Campbell, K. A.; Yikilmaz, E.; Grant, C. V.; Gregor, W.; Miller, A.-F.; Britt, R. D. *J. Am. Chem. Soc.* **1999**, *121*, 4714–4715.
(29) Campbell, K. A.; Force, D. A.; Nixon, P. J.; Dole, F.; Diner, B. A.; Britt, R. D. *J. Am. Chem. Soc.* **2000**, *122*, 3754–3761.
(30) Campbell, K. A.; Lashley, M. R.; Wyatt, J. K.; Nantz, M. H.; Britt, R. D. *J. Am. Chem. Soc.* **2001**, *123*, 5710–5719.
(31) Groni, S.; Hureau, C.; Guillot, G.; Blondin, G.; Duboc, C.; Blain, G.; Anxolabéhère-Mallart, E. Manuscript in preparation.

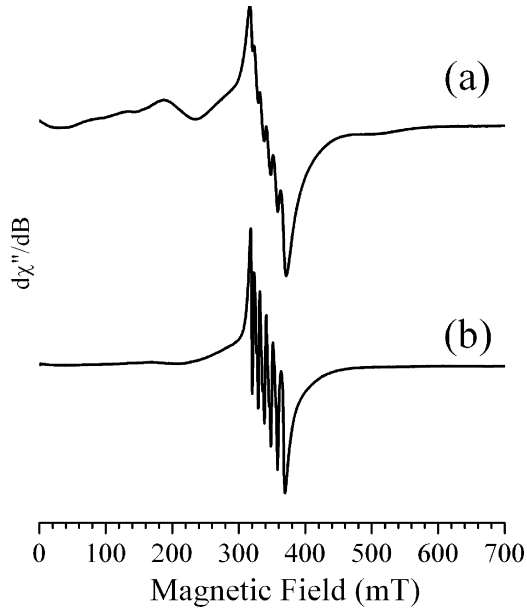

Figure 2. EPR spectra recorded in the perpendicular mode for $[LMn^{II}]^{2+}$ (a) before and (b) after addition of excess of H_2O_2 (1000-fold excess). Conditions: $C = 5$ mM, $\nu_{mw} = 9.63$ GHz, modulation amplitude 0.5 mT for (a) and (b); microwave power 2 mW (a) and 8 mW (b); $T = 10$ K (a) and 5 K (b).

addition of 250-fold excess of H_2O_2.[32] A well-defined band at 611 nm and a shoulder at 436 nm are growing over 10 min. The spectrum remains unchanged over about 30 min before slowly decaying. We reported a similar spectrum in our previous work using KO_2 as oxidant.[22] The appearance of a blue color has also been previously mentioned in the case of a related aminopyridine pentadentate ligand derived from 1,4,7-triazacyclononane with H_2O_2 as oxidant; however, it was not the subject of that study.[33]

ESI-MS data of the 5 mM solution of the $[LMn^{II}]^{2+}$ species display a peak at *m*/*z* 501, which is attributed to the monocation $\{[LMn^{II}](ClO_4)\}^+$ (Figure S1 in the Supporting Information). The ESI-MS spectrum of the blue-green solution shows the disappearance of the peak at *m*/*z* 501 and the appearance of a new peak at *m*/*z* 434. This new peak is attributed to the monocationic species $[LMn^{III}(OO)]^+$.

The evolution of a 5 mM solution of $[LMn^{II}]^{2+}$ upon addition of excess of H_2O_2 (1000-fold excess) was also followed by EPR spectroscopy in the perpendicular as well as parallel mode detection (Figures 2 and 3). The perpendicular mode EPR spectrum of the initial 5 mM solution of $[LMn^{II}]^{2+}$ exhibits broad resonances over a wide magnetic field range around $g = 9.0$ (76 mT), 5.0 (138 mT), 3.6 (191 mT), 2.0 (344 mT, with 6-line hyperfine splitting of 9.0 mT), and 1.4 (491 mT) (Figure 2a). This spectrum is characteristic of a mononuclear Mn(II) system with significant ZFS.[34,35,31] Upon addition of 1000 equiv of H_2O_2, the initial spectrum vanishes and the only detectable signal appears at $g = 2$ with a six-line hyperfine structure separated by 9.7 mT

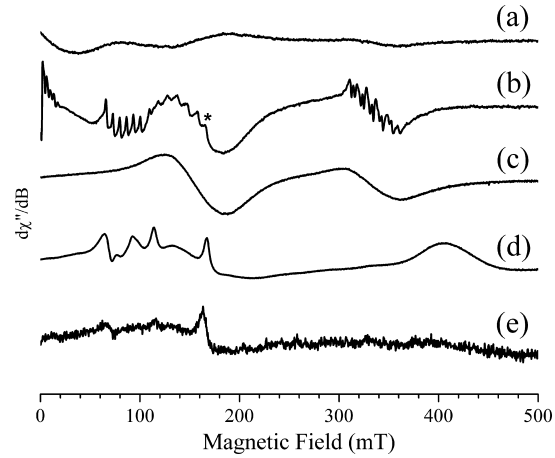

Figure 3. EPR spectra recorded in the parallel mode for $[LMn^{II}]^{2+}$ (a) before and (b) after addition of a 1000-fold excess of H_2O_2, (c) $[Mn^{II}(H_2O)_6]^{2+}$, (d) liquid O_2 from condensed air, and (e) O_2 dissolved in H_2O/MeCN solution. Experimental conditions: $C = 5$ mM (a−c); $\nu_{mw} = 9.4$ GHz; modulation amplitude 0.5 mT; microwave power 2 mW (a, e), 8 mW (b), and 0.8 mW (c, d); $T = 10$ K (a), 5 K (b−e).

(Figure 2b). This is typical of $[Mn^{II}(H_2O)_6]^{2+}$, the amount of which was found to be 8% of the total amount of Mn ion (see the Experimental Section for quantification). The above data show that the predominant species formed upon oxidation by H_2O_2 are silent in perpendicular mode EPR. Parts a and b of Figures 3 show the parallel mode EPR spectra of the same samples. The initial $[LMn^{II}]^{2+}$ species spectrum exhibits weak and broad signals from 0 to 500 mT. After addition of H_2O_2, new signals with hyperfine structures appear at zero field, $g = 8.1$ (82 mT), $g = 5.1$ (130 mT), and $g = 2.0$ (340 mT).

The resonance at zero field exhibits a hyperfine splitting of 3.5 mT. Such an hyperfine splitting favors attribution of the signal to homovalent Mn(III)Mn(III) or Mn(IV)Mn(IV) dinuclear complexes with a weak magnetic coupling between the two Mn ions rather than Mn(II)Mn(II) dinuclear complexes, which would have larger hyperfine splitting values (∼4.4 mT).[36–44] Formation of homovalent dimers upon addition of H_2O_2 to Mn complexes has already been proposed in the literature.[45] The resonance at $g = 2.0$ arises from

(32) See the Experimental Section for the choice of 250 or 1000 equiv of H_2O_2.

(33) Brudenell, S. J.; Spiccia, L.; Bond, A. M.; Fallon, G. D.; Hockless, D. C. R.; Lazarev, G.; Mahon, P. J.; Tiekink, E. R. T. *Inorg. Chem.* **2000**, *39*, 881–892.

(34) Hureau, C.; Blondin, G.; Charlot, M.-F.; Philouze, C.; Nierlich, M.; Césario, M.; Anxolabéhère-Mallart, E. *Inorg. Chem.* **2005**, *44*, 3669–3683.
(35) Policar, C.; Knüpling, M.; Frapart, Y.-M.; Un, S. *J. Phys. Chem. B* **1998**, *102*, 10391–10398.
(36) Marthur, P.; Crowder, M.; Dismukes, G. C. *J. Am. Chem. Soc.* **1987**, *109*, 5227–5233.
(37) Kessissoglou, D. P.; Butler, W. M.; Pecoraro, V. L. *Inorg. Chem.* **1987**, *26*, 495–503.
(38) Mikuriya, M.; Fujii, T.; Kamisawa, S.; Kawasaki, Y.; Tokii, T.; Oshio, H. *Chem. Lett.* **1990**, 1181–1184.
(39) Gultneh, Y.; Farooq, A.; Liu, S.; Karlin, K. D.; Zubieta, J. *Inorg. Chem.* **1992**, *31*, 3607–3611.
(40) Pessiki, P. J.; Khangulov, S. V.; Ho, D. M.; Dismukes, G. C. *J. Am. Chem. Soc.* **1994**, *116*, 891–897.
(41) Howard, T.; Telser, J.; DeRose, V. J. *Inorg. Chem.* **2000**, *39*, 3379–3385.
(42) Baffert, C.; Collomb, M.-N.; Deronzier, A.; Kjærgaard-Knudsen, S.; Latour, J.-M.; Lund, K. H.; McKenzie, C. J.; Mortensen, M.; Preuss Nielsen, L.; Thorup, N. *Dalton Trans.* **2003**, 1765–1772.
(43) Blanchard, S.; Blain, G.; Rivière, E.; Nierlich, M.; Blondin, G. *Chem. Eur. J.* **2003**, *9*, 4260–4268.
(44) Blanchard, S.; Blondin, G.; Rivière, E.; Nierlich, M.; Girerd, J.-J. *Inorg. Chem.* **2003**, *42*, 4568–4578.

$[Mn^{II}(H_2O)_6]^{2+}$, also detected in perpendicular mode. By comparison with the signal recorded from a freshly prepared $[Mn^{II}(H_2O)_6]^{2+}$ solution (see Figure 3c), the derivative line shape envelope centered at $g = 4.0$ (160 mT) is also attributed to $[Mn^{II}(H_2O)_6]^{2+}$. The sharp peak at 165 mT (indicated with an asterisk in Figure 3b) is due to the presence of O_2 in the solution. For comparison, the parallel mode EPR spectra of O_2 from liquefied air as well as from a water/MeCN solution saturated with air are shown in parts d and e of Figure 3, respectively.

In order to complete the attribution of the signals at $g = 8.1$ (82 mT, with six-line hyperfine splitting of 6.9 mT) and $g = 5.1$ (130 mT, with six-line hyperfine splitting of 9.5 mT), we investigated the evolution of the spectroscopic signatures of the blue-green solution by changing the basicity of the medium.

Addition of Base. Upon addition of 2 equiv of triethylamine $(Et)_3N$ to the blue-green solution, a change of color from blue-green to turquoise blue is observed, as well as a strong O_2 evolution. The UV–vis spectrum change is shown in Figure 1 (long dotted line). A slight shift of the λ 611 nm band is observed toward the lower wavelength (λ 609 nm), together with a global decrease of the absorption value. In addition, the shoulder at λ 436 nm vanishes. This UV–vis spectrum is closely similar to the spectrum we previously reported for the $[LMn^{III}(OO)]^+$ peroxo complex formed upon addition of KO_2 to a solution of $[LMn^{II}]^{2+}$ (λ 590 nm, $\epsilon = 165\ M^{-1}\ cm^{-1}$), for which the visible absorption band was attributed to a d−d transition of the Mn(III) ion, considering the low value of the molar extinction coefficient.[22] A similar absorption band around 590 nm has been reported in the literature for non-porphyrinic Mn(III) peroxo complexes.[19,21]

ESI-MS was recorded on the turquoise blue solution and displayed a peak at *m*/*z* 434 attributed to the monocationic species $[LMn^{III}(OO)]^+$.

The EPR spectrum of the turquoise blue solution (addition of 2 equiv of $(Et)_3N$) recorded at 5 K in the parallel mode shows the disappearance of the 6-line signal at $g = 5.1$ and the persistence of the $g = 8.1$ and zero-field signals (parts a and b of Figure 4). The disappearance of the $g = 5.1$ signal in basic medium suggests an attribution to a protonated species. The remaining $g = 8.1$ signal (82 mT, with hyperfine structure of 6.9 mT) is characteristic of a mononuclear Mn(III) complex[28–30] and is very similar to the signal that we detected previously for the $[LMn^{III}(OO)]^+$ peroxo complex obtained with KO_2. It could be simulated with a set of parameters nearly identical with those reported in our previous paper[22] (for simulation, see Figure 4c). The signal intensity decreases on increasing the temperature. This temperature dependence could be reproduced theoretically with the parameters used for the simulation of the spectrum and confirms the negative sign for D (Figure S2 in the Supporting Information).

In the perpendicular mode, the EPR spectrum recorded for the turquoise-blue solution displays a 16-line signal centered at $g = 2$ with hyperfine splitting of 8 mT and a total spectral width of 125 mT (Figure S3 in the Supporting Information). These features are characteristic of the formation of a mixed-valent di-μ-oxo Mn(III)Mn(IV) complex.[34] The quantification of this signal led to the estimation of a 0.4 mM concentration for the mixed-valent complex (16% in Mn ion). In addition, broad signals around 180 and 520 mT are also observed and attributed to the homovalent dinuclear complexes detected in the parallel mode.

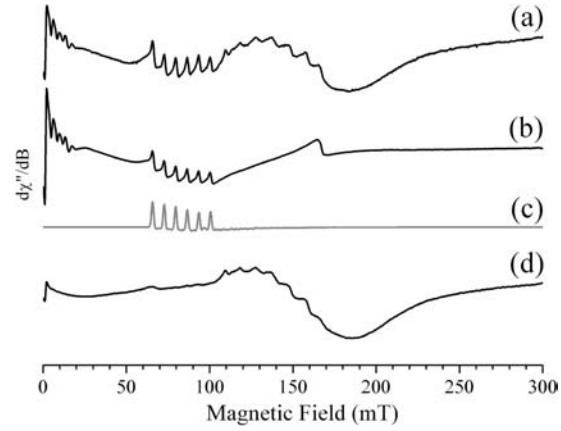

Figure 4. Zoom of the parallel mode EPR spectra in the 0–300 mT region: (a) $[LMn^{II}]^{2+}$ after addition of a 1000-fold excess of H_2O_2; (b) same as (a) after addition of 2 equiv of triethylamine $(Et)_3N$; (c) XSophe simulation of spectrum (b) with $D = -2.9\ cm^{-1}$, $E/D = 0.075$, $g_z = 2$, $A_z = 0.0065\ cm^{-1}$; (d) same as (a) after addition of 1.5 equiv of H^+ ($HClO_4$).

When the solution was abandoned in the air at room temperature, the turquoise-blue solution evolved to a brownish solution. The EPR spectrum recorded on the final solution indicated the presence of a mixed-valent di-μ-oxo Mn(III)-Mn(IV) complex.

Addition of H_2O_2 in Urea. Upon addition of 250 equiv of nonaqueous H_2O_2 as a solid in urea (see the Experimental Section), the colorless $[LMn^{II}]^{2+}$ acetonitrile solution turned turquoise-blue. The UV–vis as well as the ESI-MS spectra recorded in that case were identical with those recorded in the case of aqueous H_2O_2 in the presence of $(Et)_3N$. No spectral change was observed upon addition of $(Et)_3N$ to the blue solution. The parallel mode EPR spectrum displayed only the $g = 8.1$ signal (86 mT), with hyperfine structure of 6.9 mT. The perpendicular mode detection EPR spectrum displayed no multiline signal at $g = 2$ characteristic of the presence of a mixed-valent di-μ-oxo Mn(III)Mn(IV) complex.

We thus conclude that the addition of anhydrous H_2O_2 in the presence of urea to the $[LMn^{II}]^{2+}$ acetonitrile solution leads to the formation of the peroxo species $[LMn^{III}(OO)]^+$ as the major product. As anticipated, the absence of the $g = 5.1$ signal in the parallel mode EPR spectrum correlates with the basicity of urea in acetonitrile ($pK_a = 7.7$).[46] In addition, the anhydrous character of the medium prevents the formation of homovalent and mixed-valent dinuclear complexes.

Addition of Acid. Upon addition of 1 equiv of perchloric acid ($HClO_4$) to the blue-green solution, a change of color from blue-green to green and a slight discoloration are observed. The UV–vis spectrum evolution is shown in Figure

(45) Larson, E. J.; Pecoraro, V. L. *J. Am. Chem. Soc.* **1991**, *113*, 3810–3818.
(46) Kolthoff, I. M.; Chatooni, M. K. J.; Bhowmik, S. *J. Anal. Chem.* **1967**, *39*, 1627–1633.

Scheme 2. Proposed Reaction Scheme for the Action of H_2O_2 on $[LMn^{II}]^{2+}$ [a]

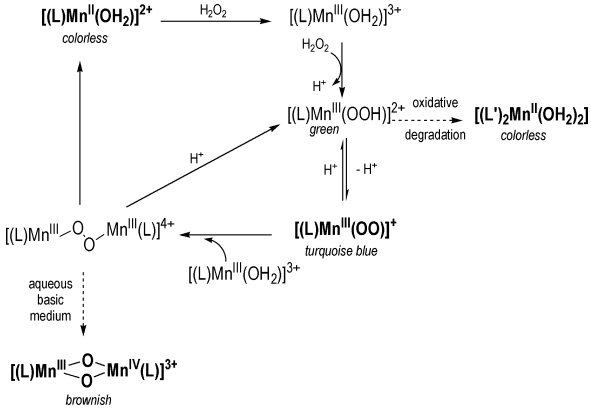

[a] Species that have been unambiguously detected are written in boldface. The other invoked species are propositions in agreement with the experimental results as discussed in the text.

1 (short dotted line). In contrast to what is observed in the case of the addition of $(Et)_3N$, the shoulder at 436 nm is conserved.

The EPR spectrum of the solution recorded at 5 K in the perpendicular mode shows only the six-line Mn(II) signal at $g = 2$. The EPR spectrum of the solution recorded at 5 K in the parallel mode shows the disappearance of the six-line signal at $g = 8.1$ and of the zero-field signals and the persistence of the derivative line shape envelope centered at $g = 4.0$ (160 mT) and of the $g = 5.1$ (132 mT, hyperfine splitting of 9.5 mT) signal (Figure 4d). As mentioned above, the resonance at zero field with hyperfine splitting of 3.5 mT is attributed to a homovalent dinuclear complex with a weak magnetic coupling between the two Mn ions. The observation that the zero-field signal disappears upon addition of proton is compatible with the breaking of an oxygenated bridge upon protonation. We propose that the homovalent dinuclear complex could be a weakly coupled peroxo bridged $Mn^{III}O-OMn^{III}$) complex (see Scheme 2).

On the basis of the behavior of the $g = 5.1$ signal upon addition of base or acid, we first considered the attribution of this signal to the protonated form $[LMn^{III}OOH]^{2+}$ species, which is a good candidate for the green coloration of the solution. It was possible to simulate this EPR signal considering a Mn(III) ion with a D value of $+2.9$ cm^{-1} and an E/D value of 0.011. The positive value of D was required to reproduce the experimental temperature dependence. The magnitude of the hyperfine splitting (9.5 mT) for this signal is also theoretically compatible with a positive D value.[29] For Mn(III) complexes detected with parallel mode EPR, the E/D values are always much larger[28–30] than that obtained in the present case. However, such a low value was required to reproduce the Mn(III) parallel mode signal at $g = 5.1$.

A hyperfine value of 9.5 mT is also characteristic of a Mn(II) ion. We thus considered the attribution of the $g = 5.1$ signal to a Mn(II) species. However, hyperfine structure was not resolved for the $[Mn^{II}(H_2O)_6]^{2+}$ acetonitrile solution (Figure 3c), even under more dilute conditions. The recording of the EPR spectra of $[Mn^{II}]^{2+}$ and of $[LMn^{II}]^{2+}$ in different media showed that the hyperfine structure resolution is drastically dependent on the solvent mixture, ending in different glass quality, and on the choice of the Mn salt. Indeed, a similar hyperfine structure matching that observed in Figure 3b at 132 mT can be detected for $[Mn^{II}(H_2O)_6]^{2+}$ and for $[LMn^{II}]^{2+}$ (see Figure S4 in the Supporting Information).[47] Although we cannot exclude the attribution of the $g = 5.1$ signal to a Mn(III) complex, the field position and hyperfine splitting of the signal are in favor of a Mn(II) monomeric complex. From the above observation, we conclude that the species responsible for the green coloration of the solution in acidic medium is not detected in EPR.

When the green solution was left at room temperature, the formation of diamond-shaped colorless crystals was observed. The quality of the crystals was good enough to allow resolution of the structure using X-ray diffraction. The structure is shown in Figure 5 and reveals a Mn(II) complex with two 2-pyridinecarboxylate ligands L′; this structure has been already reported in the literature.[48] In the present case, the formation of the ligand L′ must result from oxidative degradation of the ligand L. A similar oxidative degradation has been previously reported by Martinho et al. in the case of $[(TPEN)FeO]^{2+}$, (TPEN is the ligand identical with L, with a pyridine arm in place of the methyl group).[49] In the present case we also detected the mass peak at m/z 408, corresponding to the cation $\{[(Lim)Mn^{II}](ClO_4)\}^+$, where Lim results from the loss of one pyridine arm from the ligand L ($C_{15}H_{18}N_4O_4MnCl$) (Figure S5 in the Supporting Information).

Even though the use of H_2O_2 as an oxidant has been known for decades in Mn chemistry and especially in the formation of Mn clusters,[50] little is known about the possible intermediates that can be encountered in solution. In this work we have shown that addition of H_2O_2 to a $[LMn^{II}]^{2+}$ acetonitrile solution, where L is a pentadentate ligand, generates a mixture of Mn(II) mononuclear species, a $[LMn^{III}OO]^+$ peroxo complex, homovalent Mn(III) or Mn(IV) dinuclear species, and mixed-valent di-μ-oxo Mn(III)Mn(IV) complexes. The presence of these intermediates has been evidenced by use of parallel and perpendicular mode EPR spectroscopy, UV–vis absorption spectroscopy and ESI-MS spectrometry. Experimental observations and analyses detailed above are summarized in Scheme 2 for the action of H_2O_2 on a $[LMn^{II}]^{2+}$ solution.

Addition of H_2O_2 to the initial Mn(II) solution leads to the formation of $[LMn^{III}(OOH)]^{2+}$ and $[LMn^{III}(OO)]^+$ species. The turquoise-blue peroxo species can further reacts with $[LMn^{III}(OH_2)]^{3+}$ to form a homovalent $[LMn^{III}O-OMn^{III}L]^{4+}$ dinuclear complex.[45] In basic aqueous medium this dinuclear complex ultimately evolves to the mixed-valent $[LMn^{III}(O)_2Mn^{IV}L]^{3+}$.[31,33,34] The acidic medium prevents the formation of the oxo bridges and allows oxidation of the

(47) A similar feature was also detected in the case of the $[LMn^{II}]^{2+}$ complex generated by mixing L and anhydrous $Mn^{II}(CF_3SO_2)_2$ in MeCN solution and reported in ref 22.

(48) Okabe, N.; Koizumi, M. *Acta Crystallogr., Sect. C: Cryst. Struct. Commun.* **1998**, *54*, 288.

(49) Martinho, M.; Banse, F.; Bartoli, J.-F.; Mattioli, T. A.; Battioni, P.; Horner, O.; Bourcier, S.; Girerd, J.-J. *Inorg. Chem.* **2005**, *44*, 9592–9596.

(50) Mukhopadhyay, S.; Mandal, S. K.; Bhaduri, S.; Armstrong, W. H. *Chem. Rev.* **2004**, *104*, 3981–4026.

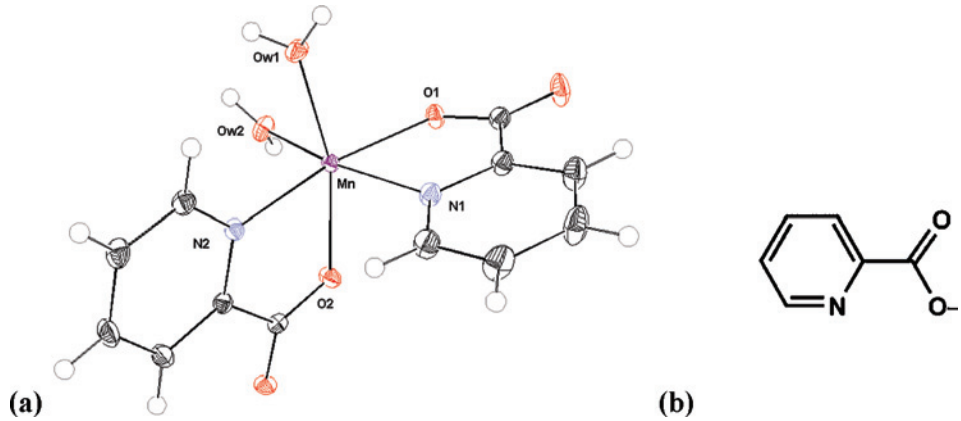

Figure 5. (a) X-ray crystallographic structure of the $[L'Mn^{II}]$ complex obtained from the degradation of $[LMn^{III}OO]^{+}$ in anhydrous medium and (b) schematic representation of 2-pyridinecarboxylate (L′).

ligand into 2-pyridinecarboxylate. This reaction route offers new opportunities for the study of the oxidation reactivity of high-oxidation-state Mn complexes. A great amount of work has been reported in the literature on the organic substrate oxidation reactivity of non-heme iron complexes.[51] In spite of in-depth mechanistic investigations of a number of systems, the nature of the reactive species is still a matter of debate. The mechanistic pathways invoke the participation of FeOOH species that can undergo either an homolytic scission of the O−O bond, thus generating Fe(IV)−oxo species and OH• hydroxyl radicals, or a heterolytic scission that would generate Fe(V)−oxo species. Non-porphyrinic Mn complexes have also been employed as catalysts using H_2O_2 as oxidant,[52–54] but characterization of the reactive species has been scarce, except in the case of complexes derived from salen[55] or salophen ligands.[56] In that latter case, spectroscopic evidence for the production of Mn(V)−oxo species upon O−O bond heterolysis of a peroxo species has been reported. In the present case we can see that a similar activation of the O−O bond occurs, thus resulting in the formation of high-valent Mn−oxo species (either Mn(IV) or Mn(V)) that would react with the ligand (thus playing the role of the substrate). Current work is focused on studying the formation of high-oxidation-state intermediates in the case of acidic medium reactivity.

Experimental Section

Chemicals. All reagents were purchased from Acros and used without further purification. H_2O_2 (35% aqueous) was titrated using $KMnO_4$ and found to be 11.6 M. White pellets of anhydrous H_2O_2 in urea were ground as a white powder prior to addition to the Mn(II) solution.

Synthesis and Solution Preparation. *N*-Methyl-*N*,*N*′,*N*′-tris(2-pyridylmethyl)ethane-1,2-diamine (L; yellow oil) was prepared according to a previously reported procedure.[31] A 0.1 M mother solution of $[LMn^{II}]^{2+}$ in acetonitrile was prepared by mixing 1 equiv of L and 1 equiv of $[Mn^{II}(H_2O)_6](ClO_4)_2$. The volume of aqueous H_2O_2 to be added is non-negligible and would generate dilution of the $[LMn^{II}]^{2+}$ solution. Thus, a typical experiment was conducted as follows: 600 μL of the 0.1 M mother solution of $[LMn^{II}]^{2+}$ (60 μmol) was diluted in 6.83 mL of acetonitrile and 1000 equiv of H_2O_2 (5.2 mL) was added, resulting in a total volume of 12 mL and a 5 mM initial solution of $[LMn^{II}]^{2+}$. For UV–vis spectroscopy experiments, only 250 equiv of H_2O_2 was added, in order to minimize O_2 bubbles and allow us to record workable spectra. However, parallel mode EPR signals were weaker in that case compared to the 1000 equiv case, indicating a lower yield of Mn(III) species formation. Therefore, the EPR spectra reported were recorded on samples prepared with 1000 equiv of H_2O_2 for signal-to-noise reasons. In addition, in the absence of an accurate concentration of Mn(III) and the presence in solution of several species (see Results and Discussion), ϵ values are not reported.

Low-Temperature Experiments and UV–Visible Spectroscopy. The solution studied was introduced into a single-envelope cell capped by using a Hellma immersion probe. Electronic absorption spectra were recorded using a Varian Cary 50 spectrophotometer connected to the Hellma immersion probe by a fiber-optic cable. The cell was cooled to −25 °C using a ThermoHaake CT90L circulation bath.

EPR Spectroscopy. X-band (9 GHz) EPR spectra were recorded on a Bruker ELEXSYS 500 spectrometer equipped with an Oxford Instrument continuous-flow liquid helium cryostat and a temperature control system. A dual mode cavity (Bruker ER 4116DM) was used for perpendicular and parallel mode detection, respectively. Both parallel and perpendicular mode detection spectra were systematically recorded on the same sample tube. An inert supporting electrolyte, tetrabutylammonium perchlorate, was added to the solution studied to a final concentration of 0.1 M in order to obtain a good glass for EPR measurements. Baseline contribution was not significant; thus, no blank spectrum was subtracted from the data. In Figures 2−4, the spectra have been arbitrarily scaled and should only be compared qualitatively.

Simulations of the EPR data were performed by using the XSophe Computer Simulation Software Suite, taking into account the temperature.[57]

Quantification of Mn(II) and Mn(III)Mn(IV). The quantity of solvated Mn(II) is estimated by comparison with spectra of

(51) Costas, M.; Chen, K.; Que, L., Jr. *Coord. Chem. Rev.* **2000**, *517*, 200–202.
(52) Brinksma, J.; Hage, R.; Kerschner, J. L.; Feringa, B. L. *Chem. Comm.* **2000**, 537–538.
(53) Brinksma, J.; Rispens, M. T.; Hage, R.; Feringa, B. L. *Inorg. Chim. Acta* **2002**, *337*, 75–82.
(54) Murphy, A.; Stack, D. T. *J. Mol. Catal. A: Chem.* **2006**, *251*, 78–88.
(55) Feichtinger, D.; Plattner, D. A. *Angew. Chem., Int. Ed. Engl.* **1997**, *36*, 1718–1719.
(56) Liu, S.-Y.; Soper, J. D.; Yang, J. Y.; Rybak-Akimova, E. V.; Nocera, D. G. *Inorg. Chem.* **2006**, *45*, 7572–7574.
(57) Hanson, G. R.; Gates, K. E.; Noble, C. J.; Griffin, M.; Mitchell, A.; Benson, S. *J. Inorg. Biochem.* **2004**, *98*, 903–916.

varying concentrations of pure species of solvated Mn(II). The quantity of mixed-valent Mn(III)Mn(IV) di-μ-oxo complex was estimated by comparison with spectra of authentic $[LMn^{III}O_2Mn^{IV}L]^{3+}$ compounds of known concentration (L = *N*,*N*′-methyl-*N*,*N*′-bis(2-pyridylmethyl)ethane-1,2-diamine) recorded under the exact same experimental conditions.

Positive-Ion ESI Mass Spectrometry. Spectra were acquired on a Quattro II (Micromass, Waters, Manchester, UK) triple-quadrupole instrument. The parameters used were set as follows: capillary voltage 3.7 kV, cone voltage 40 V, and flow rate 10 μL min^{-1}. The concentration of the injected solution was about several millimolar in pure acetonitrile. Commercially available $H_2{}^{18}O_2$ is only 0.8% and therefore prohibited isotopic labeling, considering the use of at least 250 equiv.

X-ray Crystallography. X-ray diffraction data were collected by using a Kappa X8 APPEX II Bruker diffractometer with graphite-monochromated Mo Kα radiation (λ = 0.710 73 Å). The temperature of the crystal was maintained at the selected value (100 K) by means of a Cryostream 700 series cooling device to within an accuracy of ±1 K. The data were corrected for Lorentz−polarization and absorption effects. The structures were solved by direct methods using SHELXS-97[58] and refined against F^2 by full-matrix least-squares techniques using SHELXL-97[59] with anisotropic displacement parameters for all non-hydrogen atoms. Hydrogen atoms, excepted for water molecules, were located on a difference Fourier map and introduced into the calculations as a riding model with isotropic thermal parameters. All calculations were performed by using the Crystal Structure crystallographic software package WINGX.[59] The drawing of the molecule was realized with the help of ORTEP32.[60]

Crystal data: $C_{26}H_{27}Mn_2N_5O_{12}P_2$, M_r = 711.41, monoclinic, a = 25.503(2) Å, b = 8.5136(7) Å, c = 16.8773(14) Å, α = 90°, β = 123.403(2)°, γ = 90°, V = 3059.1(4) Å^3, T = 100(1) K, space group *C*2/*c* (No. 15), Z = 8, μ(Mo Kα) = 0.895 mm^{-1}, 10 523 reflections measured, 3525 unique (R_{int} = 0.0206), 3091 ($I > 2\sigma(I)$), which were used in all calculations. Final $R(F_2)$ = 0.0249.

Crystallographic data (excluding structure factors) have been deposited at the Cambridge Crystallographic Data Center as Supplementary Publication No. CCDC-664764. Copies of the data can be obtained free of charge on application to the CCDC, 12 Union Road, Cambridge CB2 1EZ, U.K. Fax: (+44) 1223-336-033. E-mail: deposit@ccdc.cam.ac.uk.

Acknowledgment. S.G. thanks the CEA for financial support through the LCR project (LCR-CEA No.33V). The EC is thanked for financial support (STRP SOLAR-H 516510). Financial aid was provided by the French Government through the ANR NT05-443030 and the CNRS. We thank Christelle Hureau, Frédéric Banse, and Clotilde Policar for helpful discussions.

Supporting Information Available: Figures giving additional characterization data. This material is available free of charge via the Internet at http://pubs.acs.org.

IC702238Z

(58) Sheldrick, G. M. *SHELXS-97: Program for Crystal Structure Solution*; University of Göttingen, Göttingen, Germany, 1997.

(59) Sheldrick, G. M. *SHELXL-97: Program for the Refinement of Crystal Structures from Diffraction Data*; University of Göttingen, Göttingen, Germany, 1997.

(60) Farrugia, L. J. *J. Appl. Crystallogr.* **1997**, *30*, 565.